Desalination and Water Treatment
www.deswater.com

50 (2012) 157–169
December

1944-3994/1944-3986 © 2012 Desalination Publications. All rights reserved
doi: 10.1080/19443994.2012.708564

Taylor & Francis
Taylor & Francis Group

Chemical modification of coal fly ash into iodate sodalite and its use for the removal of Cd^{2+}, Pb^{2+}, and Zn^{2+} from their aqueous solutions

Ashok V. Borhade*, Arun G. Dholi, Sanjay G. Wakchaure, Dipak R. Tope

Research Centre, Department of Chemistry, HPT Arts and RYK Science College, Nasik 422005, India
Tel. +91 9421831839; email: prinhptrynsk@rediffmail.com

Received 11 March 2012; Accepted 14 May 2012

ABSTRACT

This study investigated the chemical modification of F-class coal fly ash (CFA) to an iodate enclathrated aluminosilicate sodalite, $Na_8[AlSiO_4]_6(IO_3)_2$, cubic $P\bar{4}3n$, has been synthesized by hydrothermal treatment followed by fusion of CFA with NaOH. The fused mass was mixed with excess $NaIO_3$ and hydrothermally treated at 100°C. Infrared spectroscopy, X-ray diffraction, Scanning electron microscopy, and inductively coupled plasma spectroscopy methods were used to characterize the obtained sodalite. Sorption behavior of heavy metals (Cd^{2+}, Pb^{2+}, and Zn^{2+}) from aqueous solution on iodate sodalite was examined. The Freundlich and Langmuir isotherms are evaluated for iodate sodalite. These models were fitted to the curves of heavy metals ion solutions to estimate the Freundlich (K_f) and Langmuir (Qo) adsorption parameters. These values followed the same trend of the batch experiments. The maximum sorption capacity of sodalite increased in the order $Pb^{2+} > Cd^{2+} > Zn^{2+}$ at the same condition. The effect of different parameters, such as contact time, and temperature were also investigated. The present investigation also revealed that iodate sodalite as sorbents can serve as low-cost adsorbent with higher sorption capacities towards heavy metals.

Keywords: Fly ash; Hydrothermal; Iodate sodalite; Adsorption; Heavy metals; Freundlich isotherm; Langmuir isotherm

1. Introduction

The synthesis of sodalite by hydrothermal alkaline treatment is a promising technique for the utilization of coal fly ash (CFA). Since fly ash is enriched with SiO_2 and Al_2O_3, from this waste product, various types of zeolites can be prepared, including Na-X, Na-A, zeolite 13X, zeolite Na-P, phillipsite, analcime, clinoptilolite, and chabazite [1]. Zeolite materials have been extensively employed for investigation of adsorption of heavy metals [2]. Fly ash is mainly composed of Si and Al with trace amounts of Fe, Na, K, Ca, P, Ti, and S. The major mineral compounds include amorphous aluminosilicate glass and in addition, other crystalline phases such as mullite, hematite, magnetite, lime-anhydride, and feldspars [3]. The percentages of main constituent of CFA are SiO_2 and Al_2O_3 about 70% which is classified as F-class fly ash. About 50% of fly ash is constructively utilized, but there is still a significant amount which needs to be disposed off and subsequently stored in what is called "ash dams." This type of storage has a huge land requirement. The other major problem is that, fly ash particles are considered to be highly contaminating, since their high surface area leads to potential hazards for environment. Considering the facts that, large landscapes become unusable due to fly ash waste storage, there is clearly need for

*Corresponding author.

innovative technologies to search alternative fly ash utilization. The use of fly ash for the synthesis and application [4] of high capacity ion exchange material, such as zeolites, was also quite extensively explored.

Zeolite synthesis from fly ash by several methods has been receiving a lot of attention. Holler and Barth-Wirsching [5] were the first researchers that synthesized zeolites from fly ash. A lot of investigations have been conducted to convert fly ash to zeolites. Several authors have reported the conversion of fly ash into zeolites is conventionally developed by hydrothermal crystallization under alkaline conditions. Hydrothermal synthesis [6–24] involves the treatment of 4–16 M NaOH with fly ash at a higher temperature and the incubation period is 1–6 days. The crystalline components of fly ash, quartz, and mullite cannot be dissolved substantially and remained in the fly ash at low concentration of NaOH. The fly ash zeolites cover a wide range of known zeolite frameworks and have been reviewed [25]. Recently, the conventional alkaline conversion of fly ash has been improved by using more advanced treatments, which include an alkaline fusion step followed by hydrothermal treatment. Two-step synthesis involves reacting of fly ash with sodium hydroxide at higher temperature followed by hydrothermal synthesis [26–30]. Further, it results in highly active aluminosilicate phases present in fly ash readily soluble in water and facilitated zeolite formations. The application of microwave-assisted zeolite synthesis [31] resulted in a drastic reduction of the reaction time, and a method for synthesizing zeolite under molten conditions without any addition of water [32,33].

Hydroxy-sodalite is obtained from fly ash by hydrothermal process by Henmi [9] at 100˚C for specific time with only 30% yield to hydroxy sodalite. Carlos et al. [34] also find sodalite as a major phase in the synthesis of zeolites. Clay [35], kaolin [36], metakaoline [37] are used for the synthesis of aluminosilicate sodalite. Salt enclathrated sodalite can be synthesized from fly ash by using two steps, fusion and curing hydrothermally with sodium salt. The structure of sodalite is known from early work of Pauling [38]. Sodalite has cubic symmetry and crystallizes in the space group $P\bar{4}3n$. The sodalite structure is a space-filling arrangement of identical cages having the form of truncated octahedra with inner diameter of ~6.5 Å. The sodalite framework consists of a perfectly periodic array of all-space filing [$4^6 6^8$] polyhedra, also called ß-cages or sodalite cages, formed by a network of coner-sharing TO, tetrahedra with T = Si and/or Al. Fig. 1(a) shows a single ß-cage and Fig. 1 (b) the connection of these cages by common six and four-rings. Sodalite framework containing aluminium atoms in their T sites possess a negative charge equal to the number of Al atoms, which is balanced by exchangeable metal cations present in the cages. In addition, the sodalite cages may accommodate a large variety of guest species e.g. monovalent or bivalent anions, water and organic molecules. Iodate enclathrated sodalite framework from raw CFA is considered in the present study.

Sodalite is also applied to various agricultural materials for the purpose of water purification, catalysis, soil improvement, and adsorbents [39]. Many industrial wastewater streams may contain heavy metals such as lead, cadmium, copper, arsenic, nickel, chromium, zinc, and mercury. These have been recognized as hazardous heavy metals. If the wastewaters are discharged directly into natural waters, it will constitute a great risk for the aquatic ecosystem. Heavy metal toxicity can result in significant morbidity and mortality. Heavy metals bind to oxygen, nitrogen, and sulfhydryl groups in proteins, resulting in alterations of enzymatic activity. High levels of cadmium causes both fibrotic and emphysematous lung damage but it aslo has major effect in bone and kidney. Exposure to lead, cadmium, and zinc can lead to its accumulation in liver, brain, kidney, and cornea, leading to carcinogenic danger for human life. Under typical conditions, lead is absorbed and stored in several body compartments, where it easily exchanges with the blood.

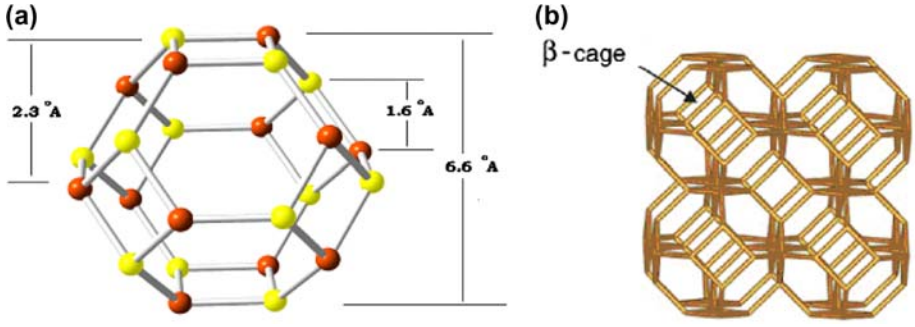

Fig. 1. Structure of (a) sodalite cage and (b) building block of the sodalite cages through connecting six- and four-rings.

In recent years, the removal of toxic heavy metal ions from sewage, industrial and mining waste effluents have been widely studied. Their presence in streams and lakes has been responsible for several types of health problems in animals, plants, and human beings [40].

Moreover, the presence of heavy metals in the environment even in moderate concentrations is responsible for illnesses related to respiratory or dermal damage and even several kinds of cancers. It is therefore important to remove toxic metal contaminant from wastewater prior to discharge as they are considered persistent and bioaccumulative. Use of zeolites synthesized from fly ash for applications in the removal of metal species from wastewaters has been a subject of study for quite some time and various investigations have been made to find the waste waters appropriate, efficient, and economical zeolite type [41–43].

Several techniques [44] such as osmosis, membrane osmosis, gravimetric precipitation, and catalytic reduction complex formation are used to remove lead, cadmium, and zinc. Sorption, one of the cost effective technique is extremely useful for the removal of heavy metals. Investigations have been conducted to convert fly ash into zeolite by hydrothermal crystallization technique. Literature survey shows that, no report is available on the conversion of raw CFA into salt-filled sodalite synthesis. In the present study, pure phase iodate sodalite is being reported for the first time by hydrothermal synthesis using CFA, including optimization of reaction conditions and detailed characterization of sodalite synthesized. In the current research, we also studied the adsorption capacities of the synthesized sodalite and its ion exchange and adsorption phenomenon for the removal of lead, cadmium, and zinc ions from wastewater. We also want to confirm whether sodalite, a dense form of zeolite is cost-effective and is an alternative sorbent that could replace the expensive resins now used for wastewater treatment.

2. Materials and methods

2.1. Iodate sodalite synthesis

Iodate sodalitel was synthesized from FA by NaOH fusion. The fresh raw CFA for the synthesis of sodalite was supplied by Eklahara thermal power plant, Nashik (India). The raw fly ash used for sodalite synthesis was analyzed by inductively coupled plasma spectroscopy for quantitative determination of its major SiO_2 and Al_2O_3 content. Table 1 presents the physico-chemical properties of the fly ash samples used in the preparation of sodalite. From the results in Table 1 it can be seen that the $[SiO_2]/[Al_2O_3]$ ratio is 1.89 for raw fly ash.

Table 1
Chemical compositions of raw fly ash

Components	Composition (wt.%)
Na_2O	00.23
Al_2O_3	29.03
SiO_2	55.00
K_2O	01.38
CaO	02.52
Fe_2O_3	07.36
MgO	00.80
Other (LOI)	03.68

The homogeneous fusion mixture was obtained by mixing pulverized FA and NaOH at 1:1 ratio. The chemical composition of fly ash and to improve the sodalite formation, the fly ash sample was subjected pre-treatment processes such as sieving and magnetic separation for removal of iron. Removing of iron from fly ash not only enhances the zeolitic property but also removes colour of zeolites. Dry fly ash and equal quantity of sodium hydroxide were mixed and fused in a steel crucible at 550°C. The resultant fused mass was cooled, milled, and mixed thoroughly in distilled water (1 g fused mass/10 mL water). 15 gm of sodium iodate salt was added in steel-lined Teflon autoclave containing aqueous mixture of fly ash and sodium hydroxide.

The Teflon autoclave was kept at 100°C for six days. The solid crystalline product was filtered and repeatedly washed with distilled water to remove excess NaOH. The obtained product dried overnight at 100°C. The schematic flow chart for the preparation of iodate sodalite is shown in Fig. 2.

2.2. Batch sorption experiment

To conduct the actual sorption experiments, the working solutions were prepared by appropriate dilution of stock solutions ($PbNO_3$, $CdNO_3$, and $ZnCl_2$) immediately prior to their use. All sorption studies with the model solutions were carried out in high density Teflon containers with a volume capacity of 100 mL, by subjecting a 0.5 g of activated sodalite to a period of shaking with 100 mL of metal ion solution and the suspension, was periodically shaken in an oven. pH was maintained at 5.00 during the experiment. Each sodalite was individually placed in separate containers and at the requisite times, the container was removed from oven and the filtrate collected by filter-

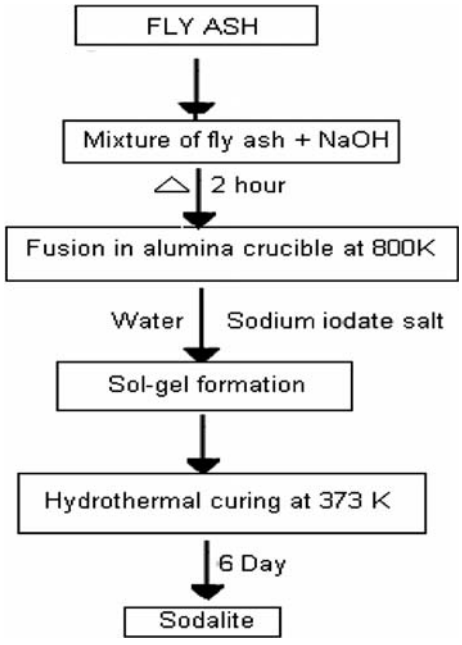

Fig. 2. Schematic diagram of formation of iodate sodalite hydrothermally at 100°C.

ing the suspension with a Whatman filter paper, after which initial and equilibrium lead and cadmium concentrations were determined with Atomic absorption spectroscopy. Zinc is determined by conventional titration with ethylenediaminetetraacetic acid (EDTA) using Erichrome black-T indicator. To study the effect of concentration on adsorption of heavy metal on sodalite, the sodalite is exposed to heavy metal ion concentrations of 20, 40, 60, 80, 100 mg/L for certain time. The volume of metal ion in each case is 100 mL and dose of adsorbate is 0.5 g. After 150 min solutions were filtered and were analyzed for adsorption capacity.

For the adsorption process, the solute transfer is due to boundary layer diffusion or intra particle diffusion or both. Various kinetic models of adsorption isotherm have been suggested for adsorption process. In this study, Langmuir and Freundlich isotherms [45–47] are evaluated for adsorption of lead, cadmium, and zinc metal ions, by iodate sodalite

Langmuir isotherm applies to adsorption on completely homogeneous surfaces with negligible interaction between adsorbed molecules. Generally, for a single pollutant, it is given by

$$Q_e = \frac{Q_o b C_e}{1 + bC_e} \quad (1)$$

Where, Q_e (mg/g) is the amount of adsorbed metal ions, C_e (mg/L) is the concentration of metal ions at equilibrium, Q_o (mg/g) is the maximum adsorption amount of metal ions and b (L/mg) is the equilibrium adsorption constant which is the related to the affinity of the binding sites.

The linear form of the equation is

$$\frac{1}{Q_e} = \frac{1}{Q_o} + \frac{1}{bQ_oC_e} \quad (2)$$

When $\frac{1}{Q_e}$ is plotted against $\frac{1}{C_e}$, a straight line having a slope of $\frac{1}{bQ_o}$ with an intercept at $\frac{1}{Q_o}$ is obtained.

For the adsorption of organic and inorganic compounds in solutions, Freundlich isotherm is very useful, which can be expressed by the following equations

$$Q_e = k_f C_e^{\frac{1}{n}} \quad (3)$$

Eq. (3) can be written in its logarithmic form as follows,

$$\mathrm{Log}Q_e = \mathrm{Log}K_f + \frac{1}{n}\mathrm{Log}\,C_e \quad (4)$$

Where Q_e is the amount adsorbed (mg/g), C_e is the equilibrium concentration of the adsorbate (mg/L), K_f and n are Freundlich constants related to the adsorption capacity and adsorption intensity, respectively. When Log Q_e is plotted against log C_e, a straight line having a slope of $\frac{1}{n}$ with an intercept at log K_f is obtained. The Freundlich and Langmuir isotherm values were obtained from the experiments.

2.3. Characterization of sodalite

2.3.1. IR spectroscopy

Infrared spectroscopy (IR) absorption analysis (KBr pellets) was performed on a Shimadzu, 8400-S FT-IR spectrophotometer in the range 4,000–400 cm^{-1}. Three types of absorption bands clearly indicate the formation of sodalite, asymmetric stretching ~1,000 cm^{-1}, symmetric stretching ~550–750 cm^{-1}, and bending vibrations ~450 cm^{-1}.

2.3.2. Powder X-ray diffraction

The phase-purity of the product was analyzed by X-ray powder diffraction pattern using a Philips PW-1710 operating at 25 kV and 25 mA using Cu-Kα radiation with wavelength $\lambda = 1.54$Å. The powder X-ray diffraction of these materials was recorded within a span of angles between 200 and 800 at 298 K. The sample was evaluated using a step size of 0.017°.

2.3.3. Magic angle spinning nuclear magnetic resonance spectroscopy

For synthesized sodalite ^{29}Si Magic-Angle Spinning Solid-State Nuclear Magnetic Resonance spectroscopy (MAS NMR) and ^{23}Na MAS NMR spectra were recorded at 130.0 MHz on a Bruker Advance 500 MHz widebore spectrometer with 6.15 μsec pulse duration, 3 s pulse delay and a spinning rate of 5 kHz in a 4 mm probe (trimetylsilane as an internal standard).

2.3.4. Scanning electron microscopy

Studies by scanning electron microscopy (SEM) were carried out to provide information about the particle morphology and crystal growth mechanism. The SEM was taken with the help of JEOL JEM-6360A model equipped with JEOL JEC 560 auto carbon coater.

3. Results and discussion

3.1. IR spectroscopy

Fig. 3(a) and (b) shows the observed IR absorption frequencies in different regions for fly ash and iodate sodalite. IR spectroscopy has also been proved to be a versatile tool not only to describe the framework type of a given aluminosilicate species, but also to characterize the enclathrated guest species. The IR spectrum of CFA of (Fig. 3(a)) clearly shows the strong absorption band due to Al–O–Si vibrations at 1,091 cm^{-1} in the mid-infrared region, whereas, Si–O is seen at 797 cm^{-1}. Absorption bands at 557 and 464 cm^{-1} are due to Al–O and Si–O respectively [48].

Detailed study of infrared spectroscopy of iodate enclathrated sodalite is also discussed elsewhere [47]. In the present study, (Fig. 3(b)) synthesized iodate sodalite from CFA shows strong band due to Al–O–Si asymmetric stretching vibrations at 988 and at 728–662 cm^{-1} is due to symmetric vibrations. Bending modes of Al–O and Si–O are located at 466–432 cm^{-1}. Apart from these framework bands enclathrated iodate characteristic sharp band is visible at 800 cm^{-1}.

3.2. X-ray analysis

The XRD pattern in Fig. 4(a) shows characteristic peaks observable in fly ash used for synthesis of sodalite. Quartz (SiO_2) and mullite ($Al_6Si_2O_{13}$) are the major phases shown in the XRD pattern (Fig. 4(a)). The presence of these phases (mullite and quartz) is very significant for the sodalite synthesis process which is the source of aluminium and silicon. After fusion and curing step, the obtained product shows sodalite pattern and is shown in the XRD pattern (Fig. 4(b)). The dissolution of SiO_2 and Al_2O_3 from quartz, mullite, and aluminosilicate glass during hydrothermal activation will result in the formation of highly crystalline sodalite. The mineral phases are identified with Joint committee on powder diffraction standards cards.

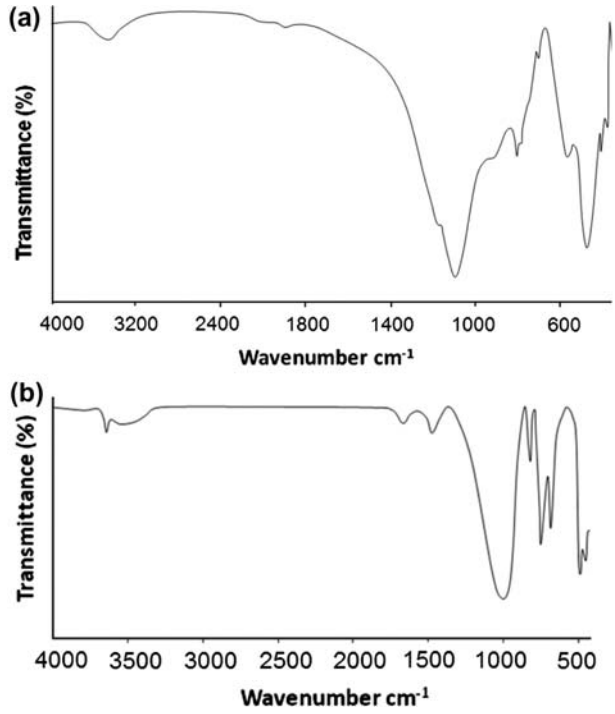

Fig. 3. IR spectra of (a) CFA and (b) iodate sodalite.

3.3. MAS NMR spectroscopy

To study the framework ordering and framework composition, MAS NMR is used. MAS NMR spectroscopy is proved to be very useful for framework species and it also gives information about non-framework species like coordination, geometry and mobility of cations and guest molecules or anions. MAS NMR spectra of ^{23}Na and ^{29}Si for iodate aluminosilicate sodalite, $Na_8[AlSiO_4]_6(IO_3)_2$, are shown in Fig. 5(a) and (b) respectively. ^{29}Si is an ideal nucleus for the study of aluminosilicate sodalite. ^{29}Si MAS NMR spectrum of a sodalite should give a single band due to perfect ordering of Si and Al in the framework. ^{29}Si chemical shift, δ, exhibits single sharp resonance line in the spectrum at −89.430, which confirms strictly alternating ordering of Si and Al atoms in the TO_4-sodalite framework, i.e. Si(4Al) units [49].

Na atoms are expected to locate above the centre of the six-ring windows of the cages and coordinated

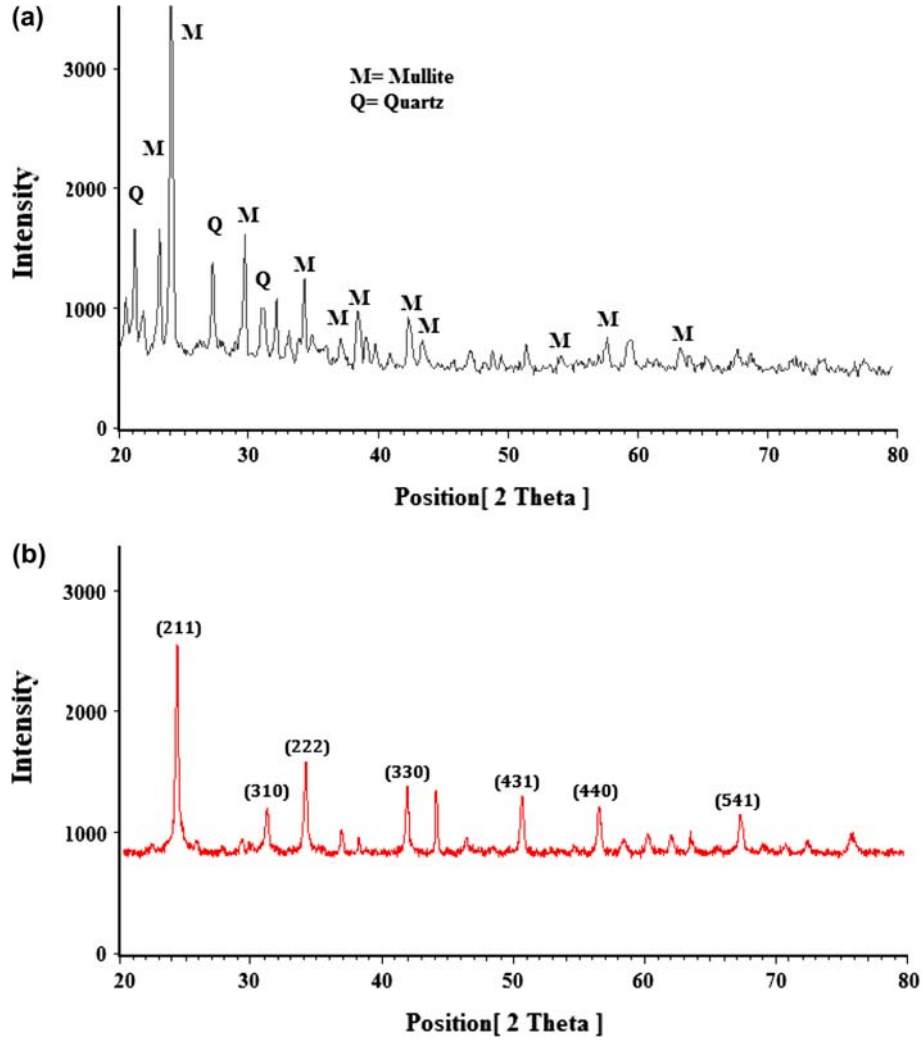

Fig. 4. XRD pattern (a) Fly ash and (b) aluminosilicate iodate sodalite.

with three oxygen atoms and anions in the sodalite cage. ^{23}Na MAS NMR spectrum of iodate sodalite gives sharp single line in the spectrum at −4.363 ppm. These results matches well with the results reported in the literature [50,51].

3.4. Scanning electron microscopy

SEM images in Fig. 6(a) illustrate several aspects about the morphology of fly ash particles. In general, fly ash particles are predominantly spherical in shape with a relatively smooth surface texture. In some cases smaller particles are attached to the surface of larger particles serving as substrate. The spherical particles are either solid or hollow. The surface morphology of the fly ash spheres usually is broken during the synthesis of iodate sodalite and shows evidence of dissolution by sodium hydroxide attack (Fig. 6(b)). Investigations of the morphology of the iodate sodalite crystals using SEM reveal relationship between the habits of the sodalite crystals. The reaction product of sodalite shows the well-known cubo-octahedral habit of synthesized iodate sodalite (Fig. 6(b)). In this case, sodalite has nearly equal size but is less perfect. After modification of fly ash with alkali it takes the cubical shape of sodalite, which indicates the completion of reaction.

3.5. Adsorbtion

In fusion process with alkali, crystalline phases are converted into sodium aluminosilicate, which is readily soluble in aqueous medium. Addition of sodium iodate to fused material enhanced the nucleation process, iodate anions act as a structure-directing agent and result in the more thermostable phase [40] like

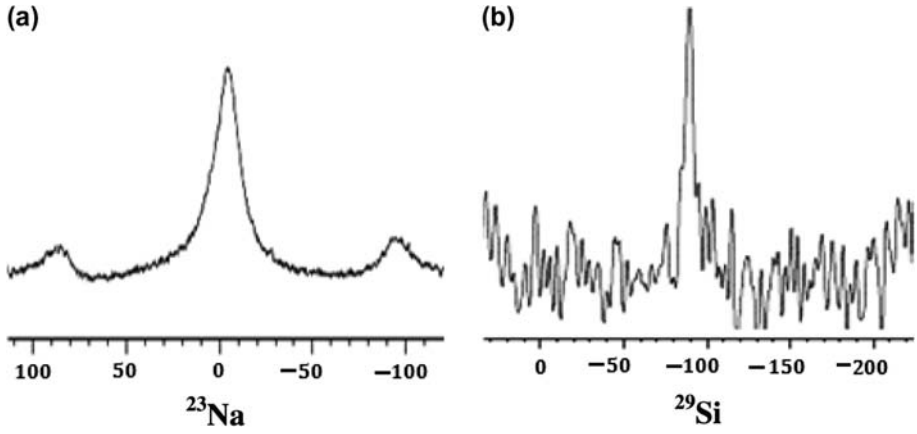

Fig. 5. MAS NMR of aluminosilicate iodate sodalite (a) ^{23}Na and (b) ^{29}Si.

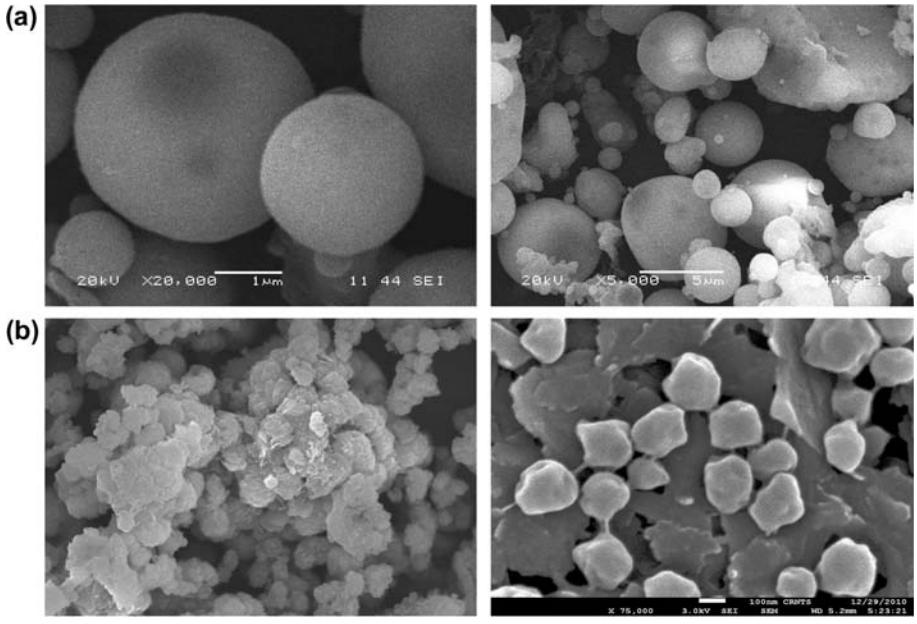

Fig. 6. SEM of (a) Fly ash and (b) SEM of aluminosilicate iodate sodalite.

sodalite. One particularly important aspect is the SiO_2/Al_2O_3 ratio in the formed sodalite, which is confirmed by ^{29}Si MAS NMR results. The low ratio increases hydrophilic nature of the sodalite and this could lead to an enhanced metal exchange capacity. The number of ions which can be sorbed or exchanged under specified experimental conditions may very well differ from the determined cation exchange capacity values, as the ion exchange capacity depend on experimental conditions and on the pore size of the sodalite.

In the present study, for every divalent metal studied (M^{2+}), the released Na^+ was in considerable excess ($\geq$twice) to the charge of metal ions exchanged onto the sodalite [52], which is a very important finding, since to maintain the equilibrium during the ion exchange process; for every metal taken up, two equivalents of Na^+ need to be released according to the following equation:

$$M^{2+} + 2Na - SOD \longleftrightarrow M - SOD + 2Na^+$$

Thus sorption is usually quite a complex process; often involving much more than simple ion exchange into the pore openings of the ion exchanger. Factors such as the pH, nature and concentration of the counter ion (metal ion), ion hydration, varying metal solubility, the presence of competing, and complexing ions

all effect the amount of metal ion that will adsorb [53]. To study these parameters; including the physical, chemical and electrostatic interactions between the sorbent (iodate sodalite material) and the sorbate (lead, cadmium, and zinc), sorption experiments were conducted with solutions consisting of selected metals.

Firstly, synthesized sodalite is leached to obtain a quantitative estimation on the expected leaching behavior of certain elements and its significance is

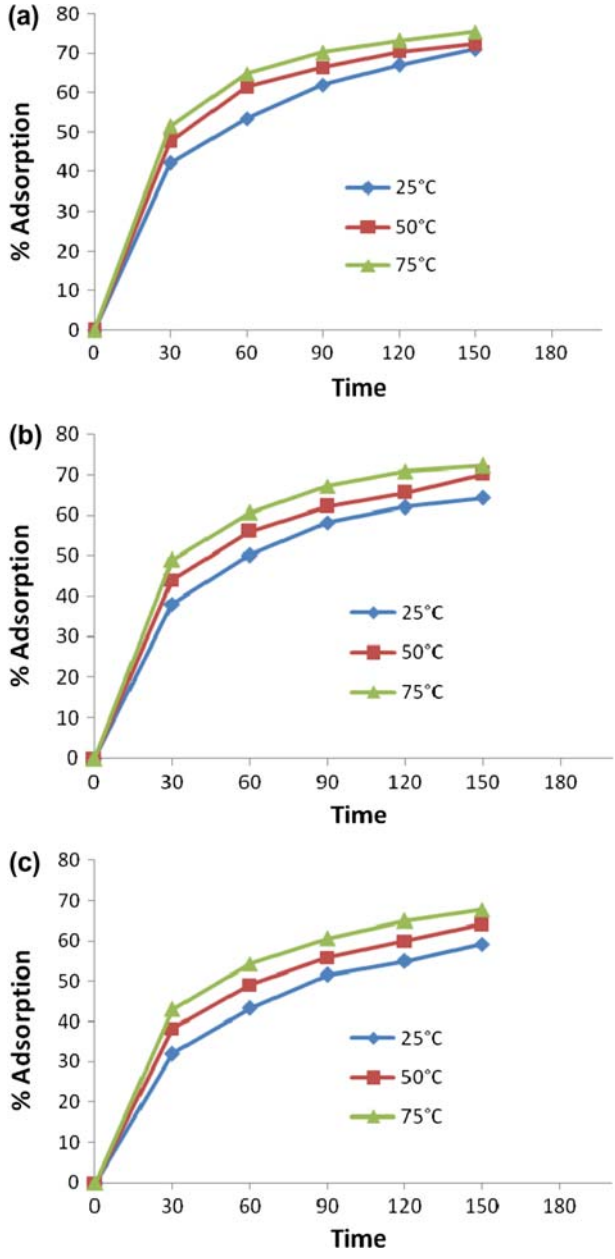

Fig. 7. Effect of contact time on the extent of adsorptions at different temperatures (a) 25˚C (b) 50˚C (c) 75˚C (Initial concentration of metals = 100 mg/L, pH = 5 and adsorbent dose = 0.5 g).

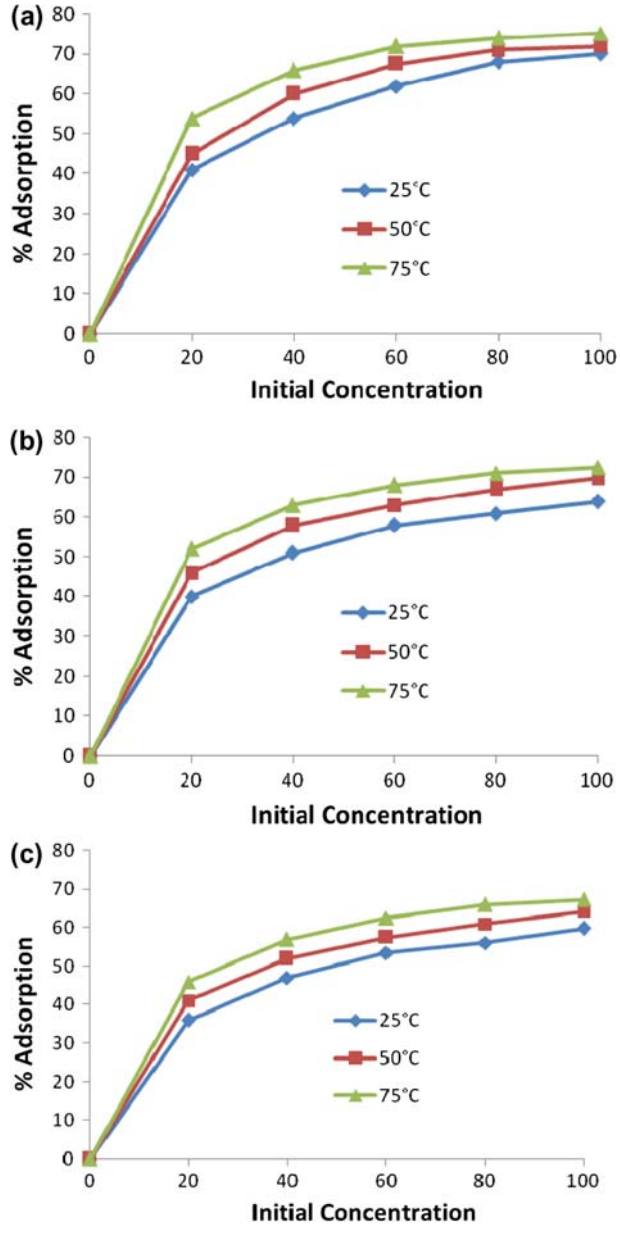

Fig. 8. Effect of Initial concentration of heavy metal ions on the extent of adsorptions at different temperatures (a) 25˚C (b) 50˚C (c) 75˚C (Initial concentration of metals = 20, 40, 60, 80, 100 mg/L, contact time = 150 min and adsorbent dose = 0.5 g).

Table 2
Metal ion characteristic parameters

Metal	Ionic radius (pm)	Hydrated radius (pm)	Electronegativity (Pauling)	Hydration enthalpy (kJ/mol)
Zn^{2+}	88	430	10.65	−2,044
Cd^{2+}	109	426	1.69	−1,806
Pb^{2+}	133	401	2.33	−1,480

Table 3
Adsorption capacities of Pb^{2+}, Cd^{2+} and Zn^{2+}, on various low-cost adsorbents

Adsorbent	Pb^{2+} mg/g	Cd^{2+} mg/g	Zn^{2+} mg/g	References
Modified kaolinite clay	40.00	13.23	27.78	[60]
Brown marine macro algae	50.40	39.50	32.00	[61]
Biofilms and associated minerals	40.00	10.40	29.40	[62]
Iodate sodalite	50.00	43.48	38.46	Present work

based on the fact that the mobility of heavy metals may cause leaching into the sodalite phase and subsequent leaching into the solution under study. The leaching result shows less than 1 ppm for all the metals under study. The potential leaching behavior of the elements may differ from one experiment to the next. Experimental and analytical error and deviation of atomic absorption spectrometry and EDTA titration is of ±2% with respect to each metal.

3.5.1. Results for contact time with sodalite and heavy metal ions

These experiments were conducted to investigate the sorption kinetics of selected metals onto the sodalite, the optimum time for the metal-sodalite system to reach equilibrium was determined. In our experiment, in 120 min. the equilibrium is attained. This is may be due to dense structure of sodalite. The results demonstrated that very low residual concentrations for almost all metal cations were observed within 120 min of contact and as such, sorption was virtually completed within this time period. The results showing the variation of % uptake of metal as a function of contact time. Fig. 7(a)–(c), confirms the decrease in solution metal concentration. The metal uptake (mg/g) vs. time curves shows a smooth, continuous increase to saturation, for most cations within the first 120 min, after which plateau values are obtained, suggesting the possible formation of single layer on sodalite and the ion exchange process [54,55].

3.5.2. Results for the temperature variation investigations

The effect of temperature on metal retention, for the adsorption of Cd^{2+}, Pb^{2+}, and Zn^{2+} was carried out at three different temperatures (25, 50, and 75°C). The equilibrium uptake (mg/g) of sodalite increased with temperature elevation for all metals studied. The results obtained shows that uptake for Pb^{2+}, Cd^{2+}, and Zn^{2+} uptake increased with temperature observed for iodate sodalite, suggests the process to be endothermic.

An increase in exchange temperature will cause progressive weakening of the ion-dipole forces between the exchanging ion (metal cations) and the

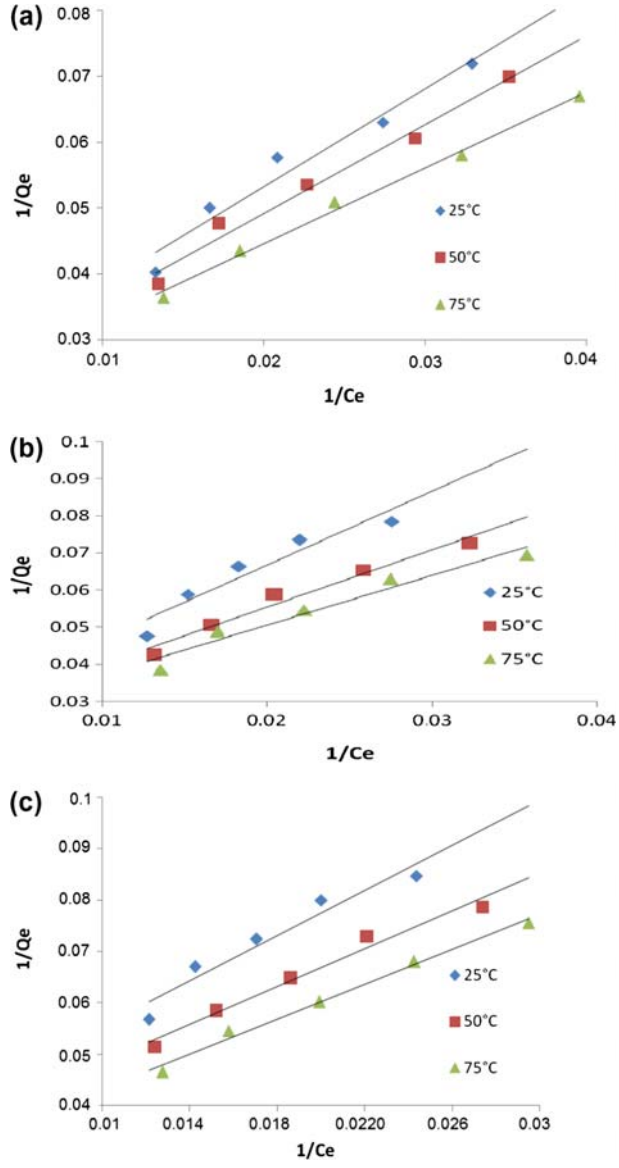

Fig. 9. Langmuir isotherms plots for adsorption of heavy metals onto iodate sodalite at 25, 50 and 75°C temperatures, (a) Pb^{2+}, (b) Cd^{2+}, (c) Zn^{2+}.

solvent dipoles (water molecules); thereby reducing the salvation coating and kinetic diameter of the ingoing metal ion and this leads to an increase in the extent of hidden site participation within the sodalite, of which the overall effect is an increase of the general affinity of the sodalite phase for the entering metal ions [56,57].

3.5.3. Results for the concentrations of heavy metal variation investigations

The relation between the initial metal ion concentration and sorption process is shown in Fig. 8(a)–(c). Metal sorption capacity of sodalite sharply increased with an increase of heavy metal ion concentration until Co of 80 mg/L. After this, Co, the metal sorption capacity remains nearly constant.

Generally, as a rule, the ion exchanger (in this case, sodalite) prefers the cation of higher valence; an effect that is purely from electrostatic forces and in many cases the smaller counter ion [54]. Hydration of the cation also plays a very significant role, since the migrating species are cation-water complexes and as such, some differences in ion exchange selectivity are bound to be attributable to necessity to reject some water molecules (see Table 2).

The metal ions with larger ionic radius have lower charge density and lower electrostatic attraction that limits the interaction of the metal ions with the adsorption sites. Thus metals with higher electronegativity sorbs more readily. The obtained selectivity series is in agreement with the metal ions electronegativity, namely Pb^{2+}(2.33)>Cd^{2+}(1.69)>Zn^{2+}(1.65). Also, with an increase of the ionic size, the absolute value of enthalpy of hydration decreases. According to the values of enthalpy of hydration, the Pb^{2+}aq ions will have a greater accessibility to the adsorbent surface [57], followed by Cd^{2+}aq and Zn^{2+}aq, which would lead to the following order Pb^{2+}>Cd^{2+}>Zn^{2+} in the extent to the adsorption process (Fig. 8(a)–(c)).

Some of the factors affecting the sorption process are hydrated radii of metal ions [58], hydration enthalpy of cations, the strength of the metal-framework oxygen bond on the zeolite type, surface the microspores of the zeolite, in this case sodalite. The order of metal ion selectivity is Pb^{2+}>Cd^{2+}>Zn^{2+}.

4. Adsorption Isotherm

Sodalites are aluminosilicates and have dense structure. They are considered to have an insignificant capability to adsorbed heavy metals. The conversion of fly ash to sodalite had a positive effect on sorption capacity due to the formation of rough surface structure with an increased surface area after the NaOH treatment favored the adsorption sorption data and were fitted to the Langmuir and Freundlich models. The adsorption [59–61] of heavy metals on different adsorbents is given for comparison in Table 3.

4.1. Langmuir isotherm

The Langmuir constants Qo and b are calculated from Fig. 9(a)–(c). Table 4 provides these values for the adsorption of Pb^{2+}, Cd^{2+} and Zn^{2+} on the iodate sodalite sample. The values of R^2 are in range 0.912–0.993 indicates that the adsorption data fit the Langmuir isotherm very well. The maximum adsorption

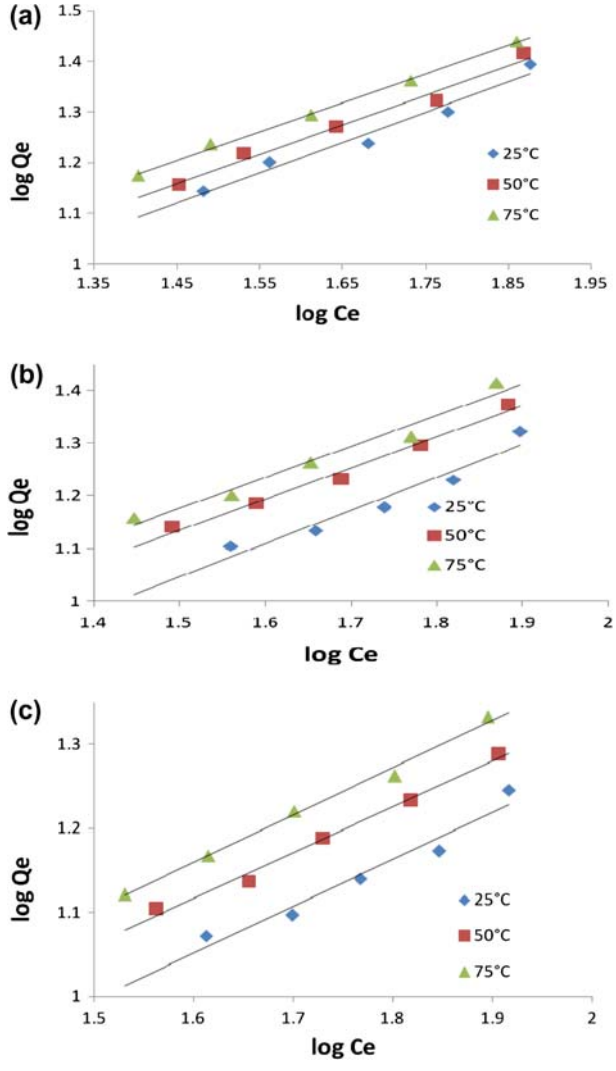

Fig. 10. Freundlish isotherms plot for adsorption of heavy metals onto iodate sodalite at 25, 50 and 75°C temperatures, different temperatures, (a) Pb^{2+}, (b) Cd^{2+}, (c) Zn^{2+}.

Table 4
Langmuir and Freundlich adsorption isotherm parameters obtained at different temperatures of Pb^{2+}, Cd^{2+}, and Zn^{2+} on iodate sodalite

Metal	Temp.	Slope	Langmuir				Slope	Freundlich			
			Intercept	b	Q_o	R^2		Intercept	n	K_f	R^2
Pb^{2+}	25	1.486	0.023	0.0155	43.48	0.959	0.597	0.254	1.675	1.794	0.968
	50	1.347	0.022	0.0163	45.45	0.981	0.583	0.312	1.715	2.051	0.983
	75	1.152	0.020	0.0174	50.00	0.993	0.565	0.348	1.770	2.228	0.997
Cd^{2+}	25	1.992	0.026	0.0131	38.46	0.912	0.628	0.103	1.592	1.260	0.935
	50	1.541	0.024	0.0156	41.67	0.969	0.592	0.246	1.689	1.761	0.993
	75	1.341	0.023	0.0172	43.48	0.951	0.589	0.291	1.698	1.954	0.966
Zn^{2+}	25	2.196	0.033	0.0150	30.30	0.933	0.558	0.158	1.792	1.438	0.953
	50	1.835	0.03	0.0163	33.33	0.978	0.544	0.245	1.838	1.757	0.991
	75	1.691	0.026	0.0154	38.46	0.989	0.564	0.256	1.773	1.815	0.993

capacities (Qo) for all the metal increase and followed the order 75°>50°>25°C.

The characteristic of Langmuir isotherm model can be described by the separation factor, R_L as follows,

$$R_L = \frac{1}{1 + b\,C_o} \tag{5}$$

Where, b is the Langmuir constant obtained from Eq. (1) and C_o is initial concentration of metal ion. The adsorption process is thermodynamically unfavorable if $R_L > 1$, linear if $R_L = 1$, thermodynamically favorable if $0 < R_L < 1$ and irreversible if $R_L = 0$. In these adsorption experiment calculated R_L values ranged from 0.3649 to 0.4329, therefore the adsorption process is thermodynamically favorable.

4.2. Freundlich isotherm

The Freundlich isotherm constants K_f and n are calculated from Fig. 10(a)–(c). Table 3 lists their values for the adsorption of Pb^{2+}, Cd^{2+}, and Zn^{2+} on the sodalite. The values of R^2 for all the metal ion adsorption are in the range 0.935–0.997, fits for Freundlich isotherm very well. n values for adsorption are greater than 1, revealing that adsorption was a favorable process.

5. Conclusions

The new process proposed in the present paper is an efficient method to obtain enclathrated sodalite from raw CFA. First time we are reporting evaluation of Langmuir and Freundlich isotherm using iodate sodalite. The present study shows that iodate aluminosilicate sodalite is an effective sorbent for the removal of cadmium, lead, and zinc ions from aqueous solutions. The sorption of Cd^{2+}, Pb^{2+}, and Zn^{2+} by sodalite is a function of the sorbet doses, initial concentration of metal ions and contact time. The results in this paper provide a good indication of the different operating conditions that would be required for efficient removal of heavy metals from aqueous solution. The obtained iodate sodalite is a dense material and its adsorption capacity is half of natural zeolite, but it shows higher adsorption capacity than reported for many adsorbents in literature, its high sorption capacity per unit cost makes this material promising and economical alternative.

Acknowledgments

Authors are thankful to UGC, New Delhi, for financial support, HPT Arts and RYK Science College, Nashik, for proving necessary facility. AGD is thankful to SAIF, IIT Pawai and Dr. S.V. Mahajan, Head, Physics Department for providing XRD Analysis.

References

[1] V. Wang, F. Lin, Synthesis of high capacity cation exchanger from a low grade Chinese natural aeolite, J. Hazard. Mater. 166 (2009) 1014–1019.
[2] E. Alvarez-Ayuso, A. Garcia-Sanchez, X. Querol, Purification of metal electroplating waste waters using zeolites, Water Res. 37 (2003) 4855–4862.
[3] A. Dabrowski, Z. Hubicki, P. Podko, S.E. Robens, Selective removal of the heavy metal ions from waters and industrial wastewaters by ion-exchange method, Chemosphere 56 (2004) 91–106.
[4] Y. Kato, K. Kakimoto, H. Ogawa, M. Tomari, Application of hydrothermally crystallized coal ash for waste water treatment, Kogyo Yosui. 338 (1986) 37–45.
[5] H. Holler, U. Barth-Wirsching, Zeolite formation from fly ash, Fortschr. Miner. 63 (1985) 21–43.

[6] S. Mohan, R. Gandhimathi, Removal of heavy metal ions from municipal solid waste leachate using coal fly ash as an adsorbent, J. Hazard. Mater. 169 (2009) 351–359.
[7] W. Shaobin, M. Soudi, Li Li, Z.H. Zhu, Coal ash conversion into effective adsorbents for removal of heavy metals and dyes from wastewater, J. Hazard. Mater. 133 (2006) 243–251.
[8] M. Park, J. Choi, Synthesis of phillipsite from fly ash, Clay Sci. 9 (1995) 219–229.
[9] X. Querol, F. Plana, A. Alastuey, A. Lopez-Soler, J.L. Fernandez-Turiel, Synthesis of industrial minerals from fly ash, Coal Sci. Technol. 24 (1995) 1979–1982.
[10] A. Singer, V. Berkgaut, Cation exchange properties of hydrothermally treated fly ash, Environ. Sci. Technol. 29 (1995) 1748–1753.
[11] W.-H. Shih, H.-L. Chang, Z. Shen, Conversion of class-F fly ash to zeolites, Mater. Res. Soc, Symp. Proc. 371 (1995) 39–44.
[12] W.-H. Shih, H.-L. Chang, Conversion of fly ash into zeolites for ion exchange application, Mater. Lett., 28 (1996) 263–268.
[13] C. Amrhein, G. Haghnia, T. Kim, P. Mosher, R. Gagajena, T. Amanios, Synthesis and properties of zeolites from fly ash, Environ. Sci. Technol. 30 (1996) 735–742.
[14] P. Catalfamo, S. Di Pasquale, F. Corigliano, L. Mavilia, Influence of the calcium content on the coal fly ash features in some innovative applications, Resour. Conserv. Recy. 20 (1997) 119–125.
[15] X. Querol, F. Plana, A. Alastuey, A. Lopez-Soler, Synthesis of Na-zeolites from fly ash, Fuel 76 (1997) 793–799.
[16] S. Rayalu, S.U. Meshram, M.Z. Hasan, Highly crystalline faujasitic zeolites from fly ash, J. Hazard. Mater. 77 (2000) 123–131.
[17] X. Querol, J.C. Umaña, F. Plana, A. Alastuey, A. Lopez-Soler, A. Medinaceli, A. Valero, M.J. Domingo, E. Garcia-Rojo, Synthesis of Na-zeolites from fly ash in a pilot plant scale: Examples of potential environmental applications, Fuel 80 (2001) 857–865.
[18] S. Rayalu, S.U. Meshram, M.Z. Hasan, Highly crystalline zeolite A from fly ash of bituminous and lignite coal combustion, J. Hazard. Mater. 88 (2001) 107–121.
[19] N. Murayama, H. Yamamoto, J. Shibata, Mechanism of zeolite synthesis from coal fly ash by alkali hydrothermal reaction, Int. J. Miner. Process 64 (2002) 1–17.
[20] Th Mouhtaris., D. Charistos, N. Kantiranis, A. Filippidis, A. Kassoli-Fournaraki, A. Tsirambidis, GIS-type zeolite synthesis from Greek lignite sulphocalcic fly ash promoted by NaOH solutions, Micropor. Mesopor. Mater. 61 (2003) 57–67.
[21] A. Molina, C. Poole, A comparative study using two methods to produce zeolites from fly ash, Miner. Eng. 17 (2004) 167–173.
[22] M. Inada, Y. Eguchi, N. Enomoto, J. Hojo, Synthesis of zeolite from coal ashes with different silica–alumina composition, Fuel 84 (2005) 299–304.
[23] K. Ojha, C. Pradhan, A. Samanta, Zeolite from fly ash: Synthesis and characterization, Bull. Mater. Sci. 27 (2004) 555–564.
[24] R. Juan, S. Hernandez, J. Andres, C. Ruiz, Synthesis of granular zeolitic materials with high cation exchange capacity from agglomerated coal fly ash, Fuel 86 (2007) 1811–1821.
[25] X. Querol, J.C. Umaña, F. Plana, A. Alastuey, A. Lopez-Soler, A. Medinaceli, A. Valero, M.J. Domingo, E. Garcia-Rojo, Synthesis of zeolites from fly ash: An overview, Int J. Coal Geol. 50 (2002) 413–423.
[26] N. Shigemoto, S. Shirakami, S. Hirano, H. Hayashi, Preparation and characterization of zeolites from coal ash, Nip. Kag. Kai. 5 (1992) 484–492.
[27] N. Shigemoto, H. Hayashi, K. Miyaura, Selective formation of Na-X zeolite from fly ash by fusion with sodium hydroxide prior to hydrothermal reaction, J. Mater. Sci. 28 (1993) 4781–4786.
[28] N. Shigemoto, S. Sugiyama, H. Hayashi, K. Miyaura, Characterization of Na-X, Na-A, and fly ash zeolites and their amorphous precursors by IR, MAS NMR and XPS, J. Mater. Sci. 30 (1995) 5777–5783.
[29] V. Berkgaut, A. Singer, High capacity cation exchanger by hydrothermal zeolitization of fly ash, Appl. Clay Sci. 10 (1996) 369–378.
[30] H. Chang, W. Shih, A general method for the conversion of fly ash into zeolites as ion exchangers for cesium, Ind. Eng. Chem. Res. 37 (1998) 71–78.
[31] X. Querol, A. Alastuey, A. López-Soler, F. Plana, M. Jose Andrés, R. Juan, P. Ferrer, C. Ruiz, A fast methodof recycling fly ash: Microwave assisted zeolite synthesis, Envir. Sci. Tech. 31 (1997) 2527–2532.
[32] M. Park, C. Choi, W. Lim, M. Kim, J. Choi, N. Heo, Molten-salt method for the synthesis of zeolitic materials: I. Zeolite formation in alkaline molten-salt system, Micropor Mesopor. Mater. 37 (2000) 81–89.
[33] M. Park, C. Choi, W. Lim, M. Kim, J. Choi, N. Heo, Molten-salt method for the of zeolitic materials: II. Characterization of zeolitic materials, Micropor. Mesopor. Mater. 37 (2000) 91–98.
[34] A. Carlos, R. Rios, C. Williams, C. Roberts, A comparative study of two methods for the synthesis of fly ash-based sodium and potassium type zeolites, Fuel 88 (2009) 1403–1416.
[35] R.M. Barrer, Zeolite and clay minerals as sorbents and molecular sieves, Academic Press, New York, NY, 1978.
[36] D. Akolekar, A. Chaffee, R. Howe, The transformation of kaoline to low-silica X zeolite, Zeolite 19 (1997) 359–365.
[37] D. Lin, X. Xu, F. Zuo, Y. Long, Crystallization of JBW, CAN, SOD and ABW type zeolite from transformation of metakaolin, Micropor. Mesopor. Mater. 70 (2004) 63–70.
[38] L. Pauling, The structure of some sodium and calcium aluminosilicates, Proc. Natl. Acad. Sci., USA 16 (1930) 453–459.
[39] R.M. Barrer, Hydrothermal chemistry of zeolites, Academic Press, London, 1982.
[40] J. Moore, S. Ramamoorty, Heavy Metals in Natural Waters: Applied Monitoring and Impact Assessment, Springer-Verlag, New York, NY, 1984.
[41] M. lee, G. Yi, B. Joon Ahn, Conversion of coal fly ash into zeolite and heavy metal removal characteristics of the products, Kor. J. Chem. Eng. 17 (2000) 325–331.
[42] B. Can, Z. Ceylan, M. Kocakerim, Adsorption of boron from aqueous solutions by activated carbon impregnated with salicylic acid: Equilibrium, kinetic and thermodynamic studies, Desalin. Water Treat. 40(1–3) (2012) 69–76.
[43] Q. Yang, J. Zhang, Q. Yang, Y. Yu, G. Yang, Behavior and mechanism of Cd(II) adsorption on loess-modified clay liner, Desalin. Water Treat. 39 (2012) 10–20.
[44] A. Krobba, D. Nibou, S. Amokrane, H. Mekatel, Adsorption of copper (II) onto molecular sieves NaY, Desalin. Water Treat. 37 (2012) 31–37.
[45] L. Langmuir, The adsorption of gases on plane surfaces of glass, mica and platinum, J. Am. Chem. Soc. 40 (1918) 1361–1403.
[46] H. Freundlish, Ueber die Adsorption in Loesungen [Over the adsorption in solution], Z. Phys. Chem. 57 (1907) 385–470.
[47] J.D. Seader, E.J. Henly, Separation Process Principles, second ed., Wiley, New York, NY, 2006.
[48] P. Khare, B. Baruah, Chemometric analysis of trace elements distribution in raw and thermally treated high sulphur coals, Fuel Process. Technol. 91 (2010) 1691–1701.
[49] G. Engelhardt, S. Lugar, J.Ch. Buhl, J. Felsche, ^{29}Si MAS n.m.r. of aluminosilicate sodalites: Correlations between chemical shifts and structure parameters, Zeolite 9 (1989) 182–186.
[50] J.-Ch. Buhl, M. Murshed, $(Na_4BH_4)^{3+}$ guests inside aluminosilicate, gallosilicate and Aluminogermanate sodalite host frameworks studied by ^{1}H, ^{11}B, and ^{23}Na MAS NMR spectroscopy, Mater. Res. Bull. 44 (2009) 1581–1585.

[51] G. Engelhardt, H. Keller, P. Sieger, W. Depmeier, A. Samoson, ^{27}A1 and ^{23}Na double rotation NMR of sodalites, Solid State Nuc. Mag. Reson. 1 (1992) 127–135.
[52] S. Eiden-Assmann, New heavy metal-hydro-sodalites containing Cd^{2+}, Ag^{+} or Pb^{2+}: Synthesis by ion-xchange and characterization, Mate. Res. Bull. 37 (2002) 875–889.
[53] J. Ikhsan, I. Johnson, J. Wells, A comparative study of the adsorption of transition metals on kaolinite, J. Colloid Interf. Sci. 217 (1999) 403–410.
[54] W. Stumm, Reactivity at the mineral-water interface: Dissolution and inhibition, J. Colloid Interf. Sci., Physicochem. Eng. Aspects 120 (1997) 143–166.
[55] M. Toyoda, Y. Nanbu, T. Kito, M. Hiranob, M. Inagaki, Preparation and performance of anatase-loaded porous carbons for water purification, Desalination, 159 (2003) 273–282.
[56] J. Inglezakis, M. Loizidou, H. Grigorpoulou, Ion exchange studies on natural and modified zeolites and the concept of exchange site accessibility, J. Colloid Interf. Sci. 275 (2004) 570–576.
[57] M. Keane, Role of alkali metal co-cation in the ion exchange of Y zeolites II. Copper ion-exchange equilibria, J. of Micropor. Mater. 3 (1995) 385–394.
[58] J. Peric, M. Trigo, N. Medvidović, Removal of zinc, copper and lead by natural zeolite—a comparison of adsorption isotherms, J. Water Res. 38 (2004) 1893–1899.
[59] D. Dong, Y. Li, J. Zhang, X. Hua, Comparison of the adsorption of lead, cadmium, copper, zinc and barium to freshwater surface coatings, Chemosphere 51 (2003) 369–373.
[60] O. Freitas, R. Martins, C. Delerue-Matos, R. Boaventura, Removal of Cd(II), Zn(II) and Pb(II) from aqueous solutions by brown marine macro algae: Kinetic modelling, J. Hazard mater. 153 (2007) 493–501.
[61] M.W. Amer, F.I. Khalili, A.M. Awwad, Adsorption of lead, zinc and cadmium ions on polyphosphate-modified kaolinite clay, J. Environ Chem. Ecotox. 2(1) (2010) 1–8.
[62] P. Mead, M. Weller, Synthesis, structure, and characterization of halite sodalite: $M_8[AlSiO_4]_6(XO_3)_x(OH)_{2-x}$; M = Na, Li, or K; X = Cl, Br, or I, Zeolite 15 (1995) 561–568.